Acta Mech Sin (2007) 23:1–9
DOI 10.1007/s10409-006-0044-3

RESEARCH PAPER

# A model for the scattering of long waves by slotted breakwaters in the presence of currents

**Zhenhua Huang · M. S. Ghidaoui**

Received: 2 June 2006 / Revised: 11 August 2006 / Accepted: 4 September 2006 / Published online: 6 January 2007


**Abstract** Slotted breakwaters have been used to provide economical protection from waves in harbors where surface waves and currents may co-exist. In this paper, the effects of currents on the wave scattering by slotted breakwaters are investigated by using a simple model. The model is based on a long wave approximation. The effects of wave height, barrier geometry and current strength on the reflection and transmission coefficients are examined by the model. The model results are compared with recent experimental data. It is found that both the wave-following and wave-opposing currents can increase the reflection coefficient and reduce the transmission coefficient. The model can be used to study the interaction between long waves and slotted breakwaters in coastal waters.

**Keywords** Wave scattering · Wave-structure interaction · Slotted breakwaters

## 1 Introduction

Breakwaters that are in the form of vertical slotted barriers have been used to provide economical protection from waves in harbors or marinas (Isaacson [1]). One example is the concrete pile breakwater at Pass Christian, Mississippi, which consists of 1.4 m diameter piles with an average spacing of 15.2 cm between piles [2]. The prediction of the wave scattering by a vertical, slotted barrier is of interest for design purposes. Extensive researches have been carried out, both theoretically and experimentally, on the interaction between the slotted structures and surface waves without the presence of currents.

Wiegel [3] and Hayashi [4] studied the scattering of waves by the pile breakwaters, and provided simple expressions for the calculation of the transmission coefficients. Kakuno and Liu [5], Yu [6] and Isaacson [1] studied, theoretically or experimentally, the interaction between waves and slotted/porous structures [7–10]. Chwang and Chan [11] reviewed the recent studies of wave–porous structure interaction. Previous studies have shown that the loss of wave energy was related to the frictional effects caused by flows through gaps between the piles or bars.

In coastal waters, surface waves and tidal currents co-exist. The surface waves may follow the tidal currents (for flood flows) or oppose the tidal currents (for ebb flows). Typically, the velocity of the tidal currents is comparable to the wave orbital velocity. Few works on the wave scattering by a slotted breakwater in the presence of a steady current were published. Rey et al. [12] experimentally studied the scattering of waves by a submerged horizontal plate. For the scattering of surface waves by a slotted barrier in the presence of currents, it is expected that currents can significantly change the hydrodynamic coefficients and affect the hydraulic performance of the breakwaters. We have not found any published theoretical work on the effects of currents on the scattering of long waves by slotted breakwaters.

The project partially supported by the Hong Kong Research Grant Council under Grant No. HKUST-DAG03/04.EG39 and HKUST6227/04E.

Z. Huang (✉) · M. S. Ghidaoui
Department of Civil Engineering, The Hong Kong University of Science and Technology, Clearwater Bay, Kowloon, Hong Kong, China
e-mail: cehzh@ust.hk

M. S. Ghidaoui
e-mail: ghidaoui@ust.hk

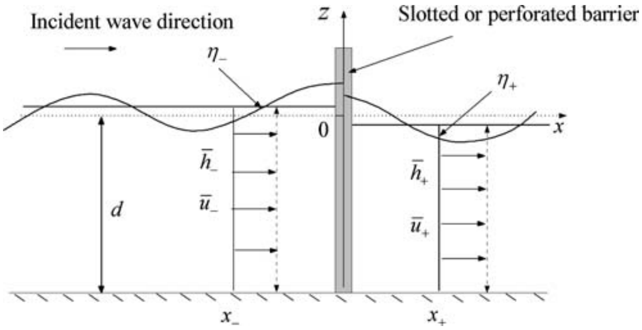


**Fig. 1** Definition sketch for the interaction between a slotted barrier and surface waves riding on a following current

In this paper, the interaction between long waves (swells) and slotted breakwaters is considered. An analytical model is presented to examine the effects of currents on the scattering of long waves by slotted breakwaters in the presence of a uniform current. The predicted transmission and reflection coefficients are compared with the experiments.

## 2 Theoretical analysis

Let the $x$ coordinate axis point in the direction of wave propagation, and the horizontal velocity in the $x$-direction is denoted by $u$. The $z$ coordinate axis points vertically upwards with its origin at the still water level. In this coordinate system, the bottom is located at $z = -d$, and the moving surface is described by $z = \eta(x,t)$ with $t$ being time. A wave barrier in the form of slotted structure of porosity $n$ is located at $x = 0$ and extends from the bottom to the surface. Long waves are considered as propagating on a current, which can be represented by a uniform current $\bar{u}$, as shown in Fig. 1. The long waves are assumed to be normal to the barrier.

### 2.1 Wave solutions in the far fields

Away from the barrier, the equations governing the long wave motion are those of long-crested shallow water waves with no bed slope or friction . The equations governing the long waves can be written as [13]

$$\frac{\partial \eta}{\partial t} + \frac{\partial (hu)}{\partial x} = 0, \tag{1}$$

$$\frac{\partial u}{\partial t} + u\frac{\partial u}{\partial x} = -g\frac{\partial \eta}{\partial x}, \tag{2}$$

where the gravitational acceleration is $g$, and the instantaneous water depth $h = d + \eta$ with $\eta$ being the surface displacement and $d$ the still water depth.

The total horizontal velocity and the total surface displacement may be written as

$$u = \bar{u} + \tilde{u}, \quad \eta = \bar{\eta} + \tilde{\eta}, \tag{3}$$

where the over-bar represents the time–mean component (averaged over one wave period) and the tilde represents the fluctuating component. The wave-induced set-up or set-down, which contributes to $\bar{\eta}$, normally is small and will be ignored in this analysis [13]. Therefore, the mean surface displacement $\bar{\eta}$ is due purely to the energy loss associated with the mean flow through the barrier. The wave-induced secondary currents, comparable to the wave-induced Stokes drift, are also ignored in this study [14,15]; thus the time-mean velocity $\bar{u}$ is the same as that in the absence of waves.

Away from the breakwaters, the nonlinear wave-wave interaction terms in Eqs. (1) and (2) can be ignored to give the following linearized governing equations [16]

$$\frac{\partial \tilde{\eta}}{\partial t} + \bar{h}\frac{\partial \tilde{u}}{\partial x} + \bar{u}\frac{\partial \tilde{\eta}}{\partial x} = 0, \tag{4}$$

$$\frac{\partial \tilde{u}}{\partial t} + \bar{u}\frac{\partial \tilde{u}}{\partial x} = -g\frac{\partial \tilde{\eta}}{\partial x}, \tag{5}$$

where the mean water depth is $\bar{h} = d+\bar{\eta}$. For long waves, the fluctuating component of the surface displacement, $\tilde{\eta}$, can be represented by

$$\tilde{\eta} = \mathrm{Re}\left(a e^{i(\omega t - \gamma k x)}\right), \tag{6}$$

where the operator Re means taking the real part of its argument. The wave angular frequency is $\omega$, the wavenumber $k$, and the wave amplitude $a$. For waves propagating in the positive $x$-direction $\gamma = 1$, otherwise $\gamma = -1$.

The fluctuating horizontal velocity $\tilde{u}$, which is associated with the surface displacement specified by Eq. (6), is found from the governing Eqs. (4) and (5) [16],

$$\tilde{u} = \mathrm{Re}\left(\frac{\gamma g k a}{\omega - \gamma \bar{u} k} e^{i(\omega t - \gamma k x)}\right) = \mathrm{Re}\left(\gamma a \sqrt{\frac{g}{\bar{h}}} e^{i(\omega t - \gamma k x)}\right). \tag{7}$$

In deriving the above expression for $\tilde{u}$, the following linear dispersion relationship for long waves is obtained,

$$(\omega - \gamma k \bar{u})^2 = g k^2 \bar{h}. \tag{8}$$

Referring to Fig. 2, the surface displacements and velocities at $x = x_-$ and $x = x_+$, which are immediately before and after the barrier, can now be written as

$$\eta_- = \bar{\eta}_- + \tilde{\eta}_-, \quad \eta_+ = \bar{\eta}_+ + \tilde{\eta}_+, \tag{9}$$

$$u_- = \bar{u}_- + \tilde{u}_-, \quad u_+ = \bar{u}_+ + \tilde{u}_+, \tag{10}$$

with

$$\tilde{\eta}_- = \mathrm{Re}\left(a e^{\mathrm{i}(\omega t - k_I x_-)} + R a e^{\mathrm{i}(\omega t + k_R x_-)}\right), \tag{11}$$

$$\tilde{\eta}_+ = \mathrm{Re}\left(T a e^{\mathrm{i}(\omega t - k_T x_+)}\right), \tag{12}$$

$$\tilde{u}_- = \frac{\sqrt{g}}{\sqrt{\bar{h}_-}} \mathrm{Re}\left(a e^{\mathrm{i}(\omega t - k_I x_-)} - R a e^{\mathrm{i}(\omega t + k_R x_-)}\right), \tag{13}$$

$$\tilde{u}_+ = \frac{\sqrt{g}}{\sqrt{\bar{h}_+}} \mathrm{Re}\left(T a e^{\mathrm{i}(\omega t - k_T x_+)}\right), \tag{14}$$

where the mean water depth at $x = x_\pm$ is $\bar{h}_\pm = d + \bar{\eta}_\pm$; $\bar{u}_\pm$ and $\bar{\eta}_\pm$ are the mean velocity and surface displacement at $x = x_\pm$; $\tilde{u}_\pm$ and $\tilde{\eta}_\pm$ are the fluctuating velocity and surface displacement at $x = x_\pm$. $R$ and $T$ are the reflection and transmission coefficients. For $|\bar{u}_\pm| < \sqrt{g\bar{h}_\pm}$ (subcritical flows), the values of wavenumber $k_I$, $k_R$ and $k_T$ are given by

$$k_I = \frac{\omega}{\sqrt{g\bar{h}_-} + \bar{u}_-}, \tag{15}$$

$$k_R = \frac{\omega}{\sqrt{g\bar{h}_-} - \bar{u}_-}, \tag{16}$$

$$k_T = \frac{\omega}{\sqrt{g\bar{h}_+} + \bar{u}_+}, \tag{17}$$

respectively, which are determined from the linear dispersion relationship, Eq. (8).

### 2.2 The matching conditions at the barrier

In the absence of currents, the expressions for the matching conditions at a slotted barrier have been given by Mei et al. [18]. The method of Mei et al. [18] is also valid for long waves riding on a uniform current, and is summarized below. Details can be found in either Mei et al. [18] or Sect. 6.1 of Mei [13] (pp. 254–268).

Referring to Fig. 2, when $|x_- - x_+| \ll d \ll L$, with $d$ being the depth of water and $L$ the wave length, the mass storage between $x_-$ and $x_+$ can be neglected so that conservation of mass gives the following condition

$$(\bar{u}_- + \tilde{u}_-)(\bar{h}_- + \tilde{\eta}_-) = (\bar{u}_+ + \tilde{u}_+)(\bar{h}_+ + \tilde{\eta}_+). \tag{18}$$

Similarly, the energy storage between $x_-$ and $x_c$ (which designates the location of the *vena contracta*) can be neglected from the energy equation, as long as $|x_- - x_c| \ll d \ll L$ holds. The energy storage was

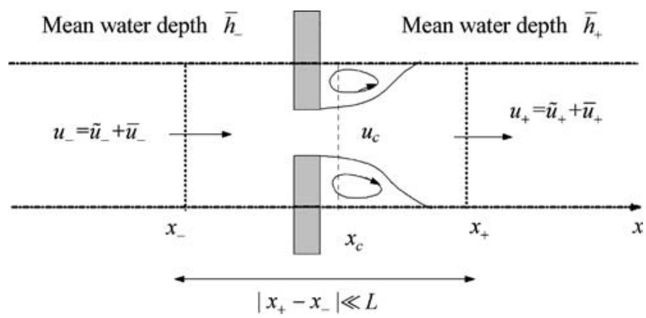


**Fig. 2** A top view of near and far fields for a typical slot taken from a slotted barrier when both $u_-$ and $u_+$ are in the direction shown in the figure

also neglected in other studies [13,17]. The energy loss associated with the turbulent jet flows between $x_c$ and $x_+$ cannot be ignored. However, because $|x_+ - x_c| \ll d \ll L$, the momentum storage and the frictional forces between $x_c$ and $x_+$ are small, and thus can be ignored when compared with the momentum flux through the cross sections of the jet flow at $x_c$ and $x_+$. By combining the energy equation between $x_-$ and $x_c$ and the momentum equation between $x_c$ and $x_+$, the following expression for the head loss due to a slotted barrier can be obtained

$$\begin{aligned}\eta_- - \eta_+ &= \frac{f}{2g}|u_+|u_+ + \frac{\ell}{g}\frac{\partial u_+}{\partial t} \\ &= \frac{f}{2g}|\bar{u}_+ + \tilde{u}_+|(\bar{u}_+ + \tilde{u}_+) + \frac{\ell}{g}\frac{\partial \tilde{u}_+}{\partial t},\end{aligned} \tag{19}$$

where the last term on the right-hand side of Eq. (19) is an inertia term, with $\ell$ being the length of the jet flow through the barrier [18]. The friction factor $f$ depends on the porosity and the shape of cylinders of the slotted barrier. The following empirical expression for $f$ was given by Mei et al. [18]

$$f = \left(\frac{1}{\epsilon C_c} - 1\right)^2,$$

where $C_c$ is the contraction coefficient of the jet flow, and needs to be determined experimentally. (A similar friction coefficient $f$ has been used in the study of waves in porous media where $f$ depends on the size and shape of solid grains and the porosity of the porous structure [7–9].) The derivation of Eq. (19) is identical to that given in Ref. [18] for the case where $\bar{u}_+ = 0$, thus will not be repeated here. However, an alternative derivation of Eq. (19) based on the concept of drag coefficient is provided in Appendix A of this paper, where it is shown that the head loss given in Eq. (19) is directly related to the wave force acting on a slotted barrier.

In this study, the friction factor $f$ used in Eq. (19) is treated as a fitting parameter. Zhu and Chwang [17] adopted the empirical expression of $f$ given by Mei et al. [18], and treated the contraction coefficient $C_c$ as a fitting parameter. These two methods are of the same empirical nature, but the former is simpler to implement. Even though the matching conditions were derived for slotted barriers, they can be used for perforated barriers as well, with $f$ being regarded as the empirical friction factor for the perforated barrier.

In deriving Eqs. (18) and (19), it was assumed that $|x_- - x_+| \ll d \ll L$ and $|x_- - x_+| = O(\ell)$ by definition [13]. Obviously, these assumption fail when the barrier is very thick. The jet length $\ell$, i.e., $|x_- - x_+|$, increases with decreasing porosity of the barrier [5]. However, the wave energy transmitted through the barrier also decreases with decreasing porosity of the barrier. Consequently, the momentum or energy flux at $x = x_-$ dominate that at $x = x_+$, and the reflection and transmission coefficients obtained by using Eqs. (18) and (20) are possibly acceptable even when the porosity is small. In practice, the porosity of slotted breakwaters is normally large enough to allow the passage of ordinary fish.

As $|x_- - x_+| \ll d \ll L$, the matching condition (19) can be asymptotically applied at $x = 0$ [13,17]. The matching condition given by Eq. (19) is nonlinear; time-mean motion and higher harmonic wave motion may be induced by the nonlinear wave–wave interaction near the barrier. From Eq. (19), the matching condition for wave motion between $x = x_-$ and $x = x_+$ can be written as

$$\tilde{\eta}_- - \tilde{\eta}_+ = \frac{f}{2g}|\bar{u}_+ + \tilde{u}_+|(\bar{u}_+ + \tilde{u}_+) + \frac{\ell}{g}\frac{\partial \tilde{u}_+}{\partial t} - \frac{f}{2g}|\bar{u}_+|\bar{u}_+, \tag{20}$$

where the last term is simply the head loss due to the steady current.

For the interaction between waves and the slotted barrier without the presence of currents, Mei et al. [18] showed that the higher harmonics, owing to the nonlinear matching condition at the barrier, contribute little to the wave reflection and transmission coefficients of the first harmonic. They also showed that the inertia term in Eq. (20) is small for long waves and can be ignored. However, in the study of the wave interaction with multiple slotted barriers, the inertia term may affect the phase of the scattered waves and the optimum chamber width at which the reflection coefficient takes its minimum [17]. Thus, in most of previous studies of wave scattering by multiple slotted walls, $\ell$ was not set to zero. In this study, the higher harmonics generated by the barrier is ignored and $\ell = 0$ is used for a single slotted barrier. Therefore, as far as the first harmonic wave motion is concerned, the matching condition (20) can be linearized by

$$\tilde{\eta}_- - \tilde{\eta}_+ = \beta\sqrt{\frac{d}{g}}\,\tilde{u}_+, \tag{21}$$

where the factor $\sqrt{d/g}$ is introduced to make the linear dissipation coefficient $\beta$ dimensionless. The linear dissipation coefficient $\beta$ needs to be determined in such a way that the losses of the wave energy predicted by Eqs. (21) and (20) are equivalent. To achieve the equivalent energy loss, $\beta$ is determined by

$$\beta = \frac{f}{2\sqrt{gd}}\frac{\overline{|\bar{u}_+ + \tilde{u}_+|(\bar{u}_+ + \tilde{u}_+)\tilde{u}_+}}{\overline{\tilde{u}_+\tilde{u}_+}}, \tag{22}$$

with the over-bar indicating the time-average over one wave period [13]. Note that the last term in Eq. (20), which is time-independent, does not contribute to the value of $\beta$ in Eq. (22). Equation (22) is called Lorentz's principle of equivalent work [7,8,13,18]. It is worth noting that if $\bar{u}_+ = 0$, the above expression for $\beta$ reduces to that given by Mei [13] for pure waves.

### 2.3 Reflection and transmission coefficients

Following Mei [13], the reflection and transmission coefficients are determined by matching the far field solutions at $x = 0$. Substituting expressions for $\tilde{u}_\pm$ and $\tilde{\eta}_\pm$ given by Eqs. (9) and (10) into the matching conditions (18) and (21), the following expressions for the reflection and transmission coefficients are obtained

$$T = \frac{2\sqrt{\left(\frac{\bar{h}_-}{d}\right)\left(\frac{\bar{h}_+}{d}\right)}}{\left(\beta + \sqrt{\frac{\bar{h}_+}{d}}\right)\left(\sqrt{\frac{\bar{h}_-}{d}} - \frac{\bar{u}_-}{\sqrt{gd}}\right) + \frac{\bar{h}_+}{d} + \frac{\bar{u}_+}{\sqrt{gd}}\sqrt{\frac{\bar{h}_+}{d}}}, \tag{23}$$

$$R = \frac{\left(\beta + \sqrt{\frac{\bar{h}_+}{d}}\right)\left(\sqrt{\frac{\bar{h}_-}{d}} + \frac{\bar{u}_-}{\sqrt{gd}}\right) - \frac{\bar{h}_+}{d} - \frac{\bar{u}_+}{\sqrt{gd}}\sqrt{\frac{\bar{h}_+}{d}}}{\left(\beta + \sqrt{\frac{\bar{h}_+}{d}}\right)\left(\sqrt{\frac{\bar{h}_-}{d}} - \frac{\bar{u}_-}{\sqrt{gd}}\right) + \frac{\bar{h}_+}{d} + \frac{\bar{u}_+}{\sqrt{gd}}\sqrt{\frac{\bar{h}_+}{d}}}. \tag{24}$$

The above expressions are exact so far, but for most of the practical problems, further approximations are possible. Note that $\bar{u}_\pm/\sqrt{gd}$ is just the Froude number for the mean flows.

When the mean flow velocity is moderate and the porosity is not too small, the change in the surface elevation associated with the head loss of the mean flow through the barrier is small, i.e., $\bar{\eta}_- = O(\bar{\eta}_+) \ll d$.

In this case, one can have the following approximations: $\bar{h}_{-} \approx d$, $\bar{h}_{+} \approx d$, $\bar{u}_{-} \approx \bar{u}$, and $\bar{u}_{+} \approx \bar{u}$ with $\bar{u} = (\bar{u}_{-} + \bar{u}_{+})/2$. Consequently, the reflection and transmission coefficients given by Eqs. (23) and (24) can be approximated by

$$T = \frac{2}{\beta(1 - \bar{u}/\sqrt{gd}) + 2},$$
$$R = \frac{\beta(1 + \bar{u}/\sqrt{gd})}{\beta(1 - \bar{u}/\sqrt{gd}) + 2}. \tag{25}$$

In view of the long wave solution given by Eq. (7) and the definition of $\beta$ given by Eq. (22), it can be seen that $\beta$ in Eq. (25) is a function of $f$, $H/d$ and $\bar{u}/\sqrt{gd}$, with $H = 2a$ being the height of the incident waves. Thus, the reflection and transmission coefficients given by Eq. (25) will be functions of $f$, $H/d$ and $\bar{u}/\sqrt{gd}$ as well.

When the mean current velocity is zero, the expressions for $T$ and $R$ given by Eq. (25) reduce to those given by Mei [13] or Yu [6] for pure waves. In coastal waters, normally the tidal current is comparable to the wave orbital velocity; thus, the difference between the mean surface elevation before and behind the barrier is usually small and the reflection and transmission coefficients given by Eq. (25) can be used in most practical designs of the slotted breakwaters with acceptable accuracy.

## 3 Results and discussion

### 3.1 Experiments

As there was no published experimental data for the wave scattering by slotted barriers in the presence of currents, a series of experiments was conducted in the Hydraulics Laboratory, HKUST, to measure the hydrodynamic coefficients of wave scattering by a slotted barrier in the presence of wave-opposing currents. The details of the experiments were reported in Ref. [19].

The length of the wave flume was 12.5 m, and the still water depth was fixed at $d = 0.3$ m ($\sqrt{gd} = 1.715$ m/s). The slotted barrier was made of aluminum bars of width 19 mm and thickness 6 mm. The porosity of the barrier was fixed at $n \approx 0.21$. A general view of the wave flume showing waves interacting with the slotted barrier is shown in Fig. 3. Two wave gages of resistance type were placed on the right side of the barrier at distances 2.1 and 2.375 m away from the barrier and one wave gage on the left 2.7 m away from the barrier (wave gages are not shown in the photo). The scattering of relative long waves by a slotted barrier was investigated for waves opposing the currents[1]. The period of the regular incident waves was fixed at $T_w = 1.1$ s in all experiments, so that the dimensionless water depth $d/L = 0.188$, with $L$ being the wave length in the absence of the current. The height of the regular incident waves ($H = 2a$) varies roughly from $H = 0.03$ m to $H = 0.07$ m for three different current velocities, $\bar{u} = 0$, $\bar{u} = -0.10$ m/s, and $\bar{u} = -0.15$ m, respectively. The dimensionless wave height varies from $H/d \approx 0.1$ to $H/d \approx 0.23$ and the three dimensionless current velocities are $\bar{u}/\sqrt{gd} = 0$, $\bar{u}/\sqrt{gd} \approx -0.06$ and $\bar{u}/\sqrt{gd} \approx -0.09$, respectively.

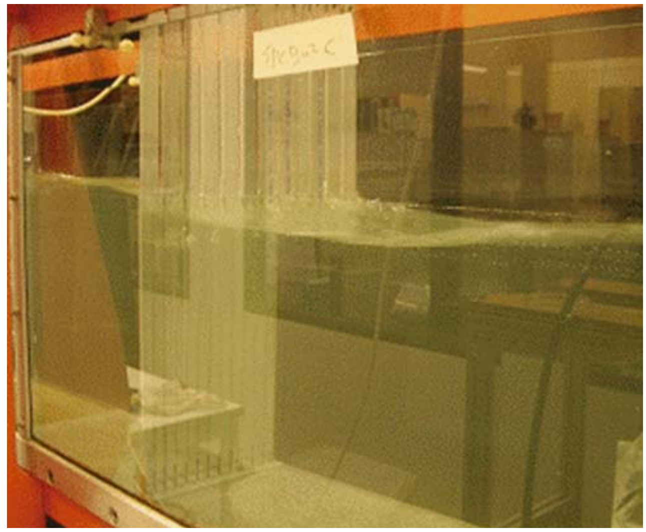

**Fig. 3** A general view of wave flume showing waves interacting with the slotted barrier in the presence of a current. Current flows from the left to the right and waves propagate from the right to the left

The measured reflection and transmission coefficients were calculated by a two-point method, which took the effects of current into account [12]. The measured reflection and transmission coefficients have a relative error less than 10%, due mainly to the reflected waves from the wave absorder at the end of the flume and the method used to separate the incident and reflected waves [20].

In the following, the predicted hydrodynamic coefficients $R$ and $T$ are compared with the measured ones. The model itself may have error when compared with the experimental data because the long wave conditions were not exactly satisfied by the laboratory conditions. In fact the error in the present model comes from two sources: (a) approximation of open-channel flow by a uniform flow, and (b) long wave approximation. Mei [13] (Sect. 6.1) compared the experimental data of Hayashi [4] with the theory based on long wave approximation, and concluded that long wave approximation

[1] Due to the limitation of the facility, there was difficulty in studying the scattering of long waves that satisfy $d/L < 1/20$.

can provide a reasonable estimation of reflection and transmission coefficients for $d/L \sim 0.16$ (which were used in the experiments of Hayashi [4]). In analyzing the present experimental data obtained for $d/L \sim 0.188$, it is believed that the aforementioned two types of errors are comparable to the error in the measured hydrodynamics coefficients.

### 3.2 Effects of current strength

Figure 4 shows a comparison between the predicted and measured reflection and transmission coefficients for the dimensionless wave height $H/d \approx 0.2$. Experiments show that the reflection coefficients increase with increasing strength of the opposing current, while the transmission coefficients decrease significantly. These trends are well captured by the theory, as indicated in Fig. 4. The predicted and measured reflection and transmission coefficients are for $\bar{u}/\sqrt{gd}=0$ and $\bar{u}/\sqrt{gd}=-0.06$. It was found that a value of $f=12.42$ provided the best fit between the measured and predicted reflection and transmission coefficients for waves alone ($\bar{u}/\sqrt{gd}=0$). As $f$ is independent of flow conditions, the same value of $f=12.42$ will be used throughout this study for all other cases where $\bar{u} \neq 0$.

Larger error exists between the predicted and measured hydrodynamic coefficients for $\bar{u}/\sqrt{gd}=-0.09$, which is not shown in Fig. 4. It was found during the experiments that the waves were quite unstable and easy to break for waves opposing the relative strong current. Therefore, it is expected that a relative large error may exist in the measured hydrodynamic coefficient for strong opposing currents.

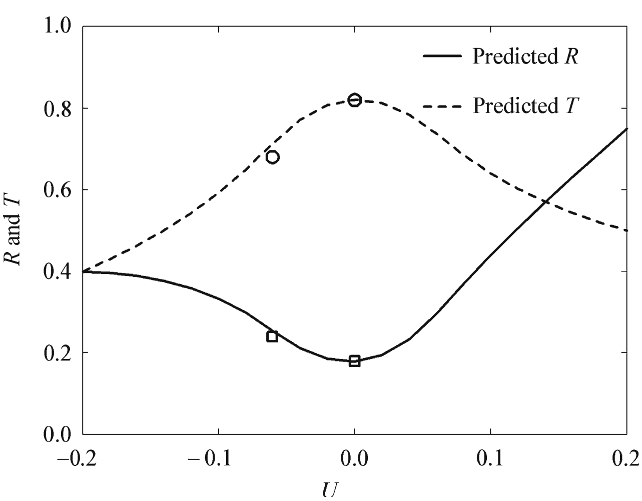


**Fig. 4** Comparison with experiments. Squares and circles are the reflection and transmission coefficients measured $U=\bar{u}/\sqrt{gd}$

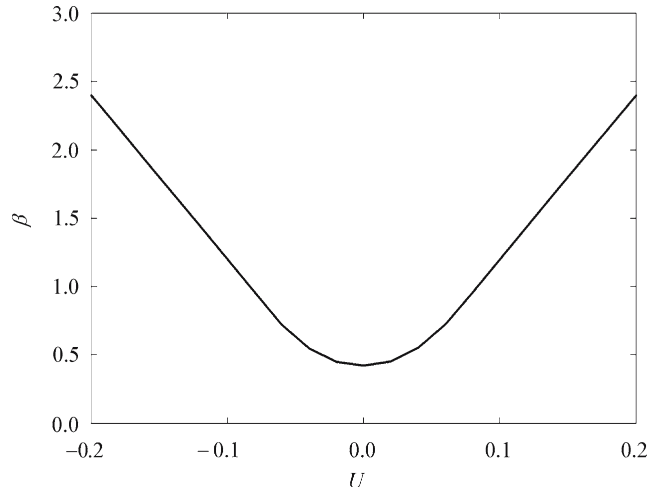


**Fig. 5** Variation of dissipation coefficient with current strength. $U=\bar{u}/\sqrt{gd}$

Figure 5 shows the variation of the linear dissipation coefficient $\beta$ with the current strength for $H/d \approx 0.2$, same as in Fig. 4. Compared with pure waves, the mean current can increase the the turbulence intensity in the neighborhood of the slotted barrier. Thus, for both the wave-following currents and the wave-opposing currents, the linear dissipation coefficient $\beta$ increases with the increasing current strength. In other words, the flow resistance and the dissipation of wave energy due to the barrier can be increased by both the wave-opposing and wave-following currents. For the example given in Fig. 4, when $|\bar{u}/\sqrt{gd}|$ is about 0.05 or larger, the dissipation coefficient varies linearly with the current strength $\bar{u}/\sqrt{gd}$, and can be approximated by $\beta \propto f|\bar{u}/\sqrt{gd}|$, i.e., $\beta$ is not affected by the wave conditions. The wave frequency and wave height will affect the linear energy dissipation coefficient only when the current is very weak relative to the waves.

### 3.3 Effects of wave height

The variation of reflection and transmission coefficients with wave height is shown in Fig. 6. The friction coefficient $f=12.42$ was used in the model for both $\bar{u}=0$ and $\bar{u}/\sqrt{gd}=-0.06$. It can be seen that the predicted $R$ and $T$ agree well with the measured. The transmission coefficient decreases with the increasing wave height, but the reflection coefficient increases. When an opposing current with a strength $\bar{u}/\sqrt{gd}=-0.06$ is present, both the reflection and transmission coefficients are insensitive to the change in the wave height. The insensitivity of $R$ and $T$ to the wave height can be explained by the observation that $\beta \propto f|\bar{u}/\sqrt{gd}|$ for $|\bar{u}/\sqrt{gd}|=0.06$ (see Fig. 5), which implies that, for a given barrier, $R$ and $T$ have a

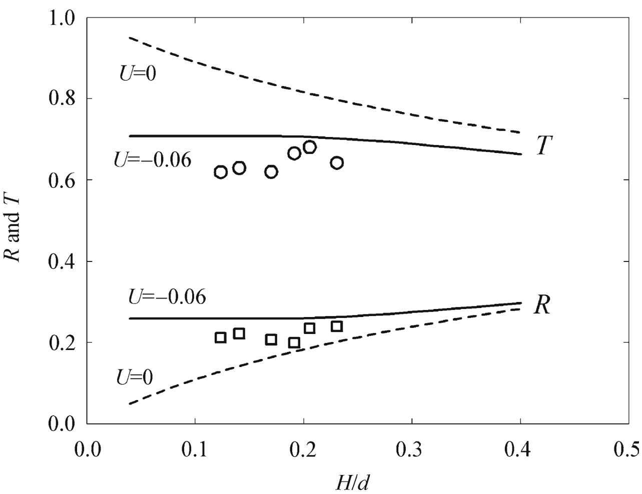


**Fig. 6** Variation of reflection and transmission coefficients with wave height. Experimental data are for $U = \bar{u}/\sqrt{gd} = -0.06$. *Squares*-measured reflection coefficients; *circles*-measured transmission coefficients. *Theory solid lines* $U = \bar{u}/\sqrt{gd} = -0.06$; *dashed lines* $\bar{u} = 0$

strong dependence on $\bar{u}/\sqrt{gd}$ and a weak dependence on the wave height.

### 3.4 Effects of the barrier geometry

No experimental data is available for the effects of barrier geometry on the reflection and transmission coefficients in the presence of currents. Here, by using the present model, the effects of frictional coefficient $f$ on the reflection and transmission coefficients when waves are riding on currents are examined. Normally, $f$ increases when the porosity of the barrier decreases.

Figure 7 shows the variation of $R$ and $T$ with the frictional coefficient $f$ for $H/d = 0.1$. For a given mean current velocity, the reflection coefficient increases with increasing $f$, but the transmission coefficient decreases. This trend is the same as that for pure waves (see e.g., Yu [6]), not affected by the presence of the current. Within the range of $f$ considered in Fig. 7, some calculated reflection coefficients for $\bar{u}/\sqrt{gd} > 0.06$ are greater than unity, which can be explained by the conservation of wave action (see, for example, Sect. 3.6 in Mei [13]). According to the conservation of wave action, the wave height may be increased by an opposing current and reduced by a following current. Therefore, for the case where the incident waves are following the current, it is possible that the height of the reflected waves is greater than that of the incident waves when the current is strong and the friction factor $f$ is large, resulting in a reflection coefficient greater than unity.

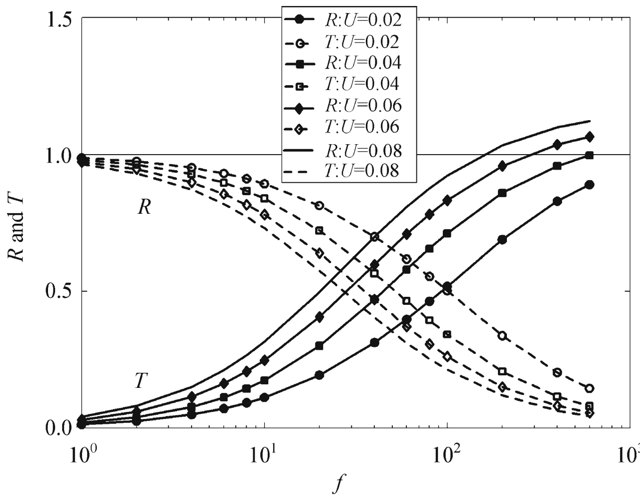


**Fig. 7** Variation of reflection and transmission coefficients with the friction coefficient $f$. $U = \bar{u}/\sqrt{gd}$

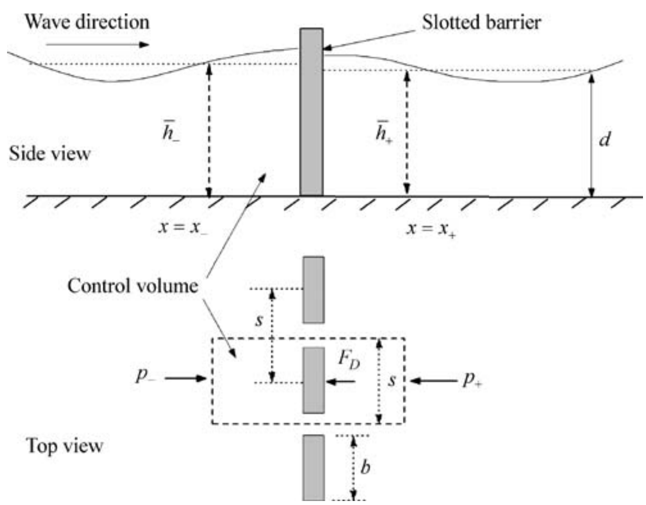


**Fig. 8** Definition sketch for the derivation of the expression for the head loss due to a slotted barrier based on the drag coefficient. The gap between two adjacent cylinders is $s - b$

## 4 Concluding remarks

An analytical model is presented to study the effects of currents on the scattering of long waves by slotted barriers in the presence of currents. The theory is based on the long wave equations without friction, and is an extension of the theory described by Mei et al. [18] for pure waves. The dissipation of wave energy caused by the barrier is modeled by a linearized dissipation coefficient determined by Lorentz's principle of equivalent work. For a moderate current strength, the predicted reflection and transmission coefficients agree reasonably well with the experimental results presented in this paper, showing that the model is promising in modeling the wave scattering by slotted barriers in the presence of a current. Model results show that both the wave-following and wave-opposing currents can increase the reflection coefficient and reduce the transmission coefficient. The model can be used to study the interaction between long waves and slotted breakwaters in coastal waters.

**Acknowledgements** The authors thank the anonymous reviewers for their constructive comments and suggestions that have greatly improved the quality of the manuscript. Mr. M. F Poon, the senior technician of the Hydraulics Laboratory at HKUST, is acknowledged for his assistance in the experiments.

## 5 Appendix

### 5.1 Derivation of the expression for the head loss due to a slotted barrier

The head loss due to a slotted barrier can also be studied by examining the wave force on a rectangular cylinder. In the following discussion, it is assumed that $|x_- - x_+| \ll d \ll L$ and the porosity, hence the gap between the two adjacent cylinders, is not zero. These two assumptions, together with the long wave approximation, have been used in deriving Eq. (19) by Mei, et al. [18].

Referring to Fig. 8, let the drag force per unit length of the cylinder be $F_D$, which can be modeled by the well-known Morison equation [21,22]

$$F_D(z,t) = \rho C_D b \frac{u_+|u_+|}{2} + \rho C_M e b \frac{\partial u_+}{\partial t}, \quad -h < z < 0, \tag{A1}$$

where $e$ is the thickness of the rectangular cylinder, $b$ the width of the cylinder, $C_D$ the drag coefficient and $C_M$ the inertia coefficient. The velocity $u_+$ is evaluated at $x = x_+$. The application of Morison equation in combined wave-current flows has been discussed by Wang et al. [23]. As $|x_- - x_+|$ is very small as compared with the water depth and the wave length, the frictional force acting on the sides of the control volume and the net momentum change in the horizontal direction can be ignored for long waves. The time rate change of the momentum in the control volume shown in Fig. 8 is balanced by the net force in $x$ direction, i.e.,

$$s(p_- - p_+) - F_D \approx \rho s |x_- - x_+| \frac{\partial u^+}{\partial t}, \tag{A2}$$

where $s$ is the spacing between the adjacent gaps and $\bar{h}_- \approx \bar{h}_+$ is assumed. Other forces in the momentum Eq. (A2) can be ignored as long as $|x_- - x_+| \ll d \ll L$. For long waves, the dynamic pressure $p$ is given by $p = \rho g \eta$, thus Eq. A2 can be written as

$$\eta_- - \eta_+ \approx C_D \frac{b}{s} \frac{u_+|u_+|}{2g} + \left( \frac{C_M}{g} e \frac{b}{s} + \frac{|x_- - x_+|}{g} \right) \frac{\partial u_+}{\partial t}. \tag{A3}$$

After comparing Eqs. 19 and A3 and noting $(s-b)/s = \epsilon$, the following two relationships are obtained

$$f = C_D(1-\epsilon), \quad \ell = e\,C_M(1-\epsilon) + |x_- - x_+|. \tag{A4}$$

Physically, the friction coefficient $f$ is related to the drag coefficient $C_D$, and the jet length $\ell$ is related to the inertia coefficient $C_M$. Similar expression for $f$ has been given by Madsen [8] for waves in porous media.

It should be noted that $C_D$ and $C_M$ for a slotted barrier are different from those for a single cylinder in an oscillatory flow, and have to be determined experimentally. Because of the relationship (A4), it is expected that, just like $C_D$, the friction factor $f$ will have a weak dependency on the Strouhal number, as suggested by Mei [13] (Sect. 6.15).

## References

1. Isaacson, M., Premasirl, S., Yang, G.: Wave interaction with vertical slotted barrier. J. Waterway Port Coast. Ocean Eng. **124**(3), 118–126 (1998)
2. Herbich, J.B.: Pile and offshore breakerwaters. In: Herbich, J.B. (ed.) Handbook of Coastal and Ocean Engineering, vol. 1, chap. 19, 895–920. Gulf Publishing Company (1990)
3. Wiegel, R.L.: Closely spaced piles as breakwater. Dock Harbour Authority **41**(491) (1961)
4. Hayashi, T., Kano, T., Shirai, M.: Hydraulic research on closely-spaced pile breakwaters. In: Proceedings of 10th Coastal Engineering Conference, vol. 2, pp. 873–884 (1966)
5. Kakuno, S., Liu, P.F.: Scattering of water waves by vertical cylinders. J. Waterway Port Coast. Ocean Eng. **119**(3), 302–322 (1993)
6. Yu, X.: Diffraction of water waves by porous breakwaters. J Waterway Port Coast Ocean Eng **121**(6), 275–282 (1995)
7. Sollitt, C.K., Cross, R.H.: Wave transmission through permeable breakwaters. In: Proceeding of 13th Conference on Coastal Engineering, 1827–1846. ASCE, Vancouver (1972)
8. Madsen, O.S.: Wave transmission through porous structures. J. Waterway Harbors. Coast. Eng. Div. **100**(3), 169–188 (1974)
9. Martin, P.A., Dalrymple, R.A.: Scattering of long waves by cylindrical obstacles and gratings using matched asymptotic expansions. J. Fluid. Mech. **188**, 465–490 (1988)
10. Huang, Z.: A method to study interactions between narrow-banded random waves and multi-chamber perforated structures. Acta Mech. Sin. **22**, 285–292 (2006)
11. Chwang, A.T., Chan, A.T.: Interaction between porous media and wave motion. Ann. Rev. Fluid Mech. **30**, 53–84 (1998)
12. Rey, V., Capobianco, R., Dulou, C.: Wave scattering by a submerged plate in presence of a steady current. Coast. Eng. **47**, 27–34 (2002)
13. Mei, C.C.: The Applied Dynamics of Ocean Surface Waves. Advanced Series on Ocean Engineering, vol 1. World Scientific, Singapore (1989)

14. Groeneweg, G., Batties, J. A.: Three-dimensional wave effects on a steady current. J. Fluid Mech. 478, 325–343 (2003)
15. Lebovich, A.: The form and dynamics of Langmuir circulation. Annu. Rev. Fluid Mech. 15, 391–427 (1983)
16. Dingemans, M.: Water wave propagation over uneven bottoms: Part 1-linear wave propagation. In: Advanced Series on Ocean Engineering, vol 13. World Scientific, Singapore (2000)
17. Zhu, S., Chwang, A.T.: Investigation on the reflection behavior of a slotted seawall. Coast Eng **43**, 93–104 (2001)
18. Mei, C.C., Liu, P.L.F., Ippen, A.T.: Quadratic head loss and scattering of long waves. J. Waterway Harbour. Coast. Eng. Div. **99**, 209–229 (1974)
19. Huang, Z.: An experimental study of wave scattering by a vertical slotted barrier in the presence of a current. Ocean Eng (2006). (In Press.) Doi 10.1016/j.oceaneng.2006.05.007
20. Goda, Y.: Random Seas and Design of Maritime Structures, 2nd edn. World Scientific, Singapore (2000)
21. Dean, R.G., Dalrymple, R.A.: Water Wave Mechanics for Engineers and Scientists. World Scientific, Singapore (1992)
22. Huhe, A., Huang, Z., Qi, G., Li, Y., Kang, H., Li, G.: Local wave forces on a vertical circular cylinder induced by regular waves. Acta Mech. Sin. **30**, 27–34 (1998) (in Chinese)
23. Wang, T., Li, J., Huhe, A., Huang, Z.: Effects of wave-current interaction on hydrodynamic coefficients. J. Hydrodyn. Series A **10**(5), 551–559 (1995) (in Chinese)